RESEARCH



How to combine multiple tools for the genetic diagnosis work-up of pediatric B-cell acute lymphoblastic leukemia

Gloria Hidalgo-Gómez^{1,2} · Bárbara Tazón-Vega¹ · Carlos Palacio¹ · Silvia Saumell¹ · Noemi Martínez-Morgado¹ · Víctor Navarro³ · Laura Murillo⁴ · Pablo Velasco⁴ · Thais Murciano⁴ · Cristina Díaz de Heredia⁴ · Francesc Bosch¹ · Gemma Armengol² · Margarita Ortega¹

Received: 21 August 2024 / Accepted: 15 December 2024 / Published online: 23 January 2025 © The Author(s) 2025

Abstract

This study investigated the importance of comprehensive genetic diagnosis in pediatric B-cell acute lymphoblastic leukemia (B-ALL). We analyzed 175 B-ALL employing karyotyping, FISH, MLPA, targeted next-generation sequencing (t-NGS), and Optical Genome Mapping (OGM). This approach achieved an 83% classification rate, identifying 17 distinct genetic subtypes. Specifically, within B-other subtype, seven different subgroups were identified (*ZNF384*, *IGH*, *DUX4*, *NUTM1* rearrangements, *PAX5* alterations, *PAX5* P80R, and *IKZF1* N159Y). Secondary genetic alterations were observed, with copy number alterations (CNA) present in 60% of cases and mutations detected in 70.6%. While these alterations exhibited specific associations with certain genetic subtypes, CNAs did not appear to significantly impact the prognosis within these genetic groups. HeH, *ETV6::RUNX1*, *ZNF384*-r, and *PAX5* P80R exhibited excellent outcomes, contrasting with the poor prognoses observed in *KMT2A*-r, hypodiploidy, and *CRLF2*-r (5-year overall OS were 50%, 50%, and 52%, respectively). These findings underscore the value of integrated genetic diagnostics for accurate subtyping, risk stratification, and guiding personalized treatment in pediatric B-ALL. Therefore, optimizing diagnostic workflows for routine clinical practice is crucial. Our study confirms the utility of conventional techniques (karyotyping and FISH), combined with t-NGS and OGM, for comprehensive genetic diagnosis.

 $\textbf{Keywords:} \ \ Acute \ lymphoblastic \ leukemia \cdot Pediatric \ ALL \cdot B-other \cdot Genetic \ diagnosis \cdot Multiple-technique \ approach$

- Margarita Ortega margarita.ortega@vallhebron.cat
- Hematology Service, Experimental Hematology, Vall d'Hebron Hospital Universitari, Vall d'Hebron Institute of Oncology (VHIO), Hospital Universitari Vall d'Hebron, Vall d'Hebron Barcelona Hospital Campus, Passeig Vall d'Hebron 119-129, 08035 Barcelona, Spain
- Unit of Biological Anthropology, Department of Animal Biology, Plant Biology, and Ecology, Faculty of Biosciences, Universitat Autonoma de Barcelona, 08193 Barcelona, Catalonia, Spain
- Oncology Data Science (ODysSey) Group, Vall d'Hebron Institute of Oncology (VHIO), Vall d'Hebron Barcelona Hospital Campus, Passeig Vall d'Hebron 119-129, 08035 Barcelona, Spain
- Pediatric Oncology and Hematology Department, Hospital Universitari Vall d'Hebron, Vall d'Hebron Barcelona Hospital Campus, Passeig Vall d'Hebron 119-129, 08035 Barcelona, Spain

Introduction

Acute lymphoblastic leukemia (ALL) is the most common childhood malignancy, and its characteristic genetic profile plays a crucial role in determining the prognosis and treatment stratification. Approximately 70% of B-cell precursor ALL (B-ALL) can be categorized using standard genetic analyses into well-established recurrent genetic abnormality [1, 2]. The remaining 30% of pediatric B-ALL, referred to as "B-other", encompasses 15 distinct genetic entities [3–6].

Current diagnostic strategies require multiple techniques. Karyotyping is the most widely used method for assessing chromosomal abnormalities, including numerical and structural variants. Fluorescence in situ hybridization (FISH) and reverse transcription polymerase chain reaction (RT-PCR) detect classical fusions. Chromosomal microarrays and multiplex ligation-dependent probe amplification (MLPA) identify specific copy number alterations (CNA), commonly observed in B-ALL patients [5]. Next generation sequencing



(NGS), such as targeted NGS (t-NGS) or whole genome sequencing (WGS), detects actionable/prognostic mutations and fusions [7]. Optical Genome Mapping (OGM) is a new technology that comprehensively detects CNA, structural variants, and fusion genes [8].

Accurately defining leukemia genetics requires a complex workflow utilizing diverse techniques; however, their accessibility varies significantly among laboratories. Our study presents a single-center cohort of ALL employing an integrated approach, which classifies patients into 17 genetic subtypes, elucidating their frequency and clinical significance. Furthermore, we aim to identify the most relevant techniques for a comprehensive genetic diagnosis.

Materials and methods

This study included 175 patients (≤18 years) with B-ALL treated at Vall d'Hebron University Hospital from 2014 to 2023 according to the Spanish SEHOP-PETHEMA 2013 protocol [9] or a similar risk-adapted regimen. Leukemia diagnosis was based on morphology, immunophenotype, cytogenetics, FISH, and RT-PCR as part of routine clinical diagnostics. Classification was made according to the 5th edition of the WHO Classification of Haematolymphoid Tumours (WHO-HAEM5) [1], which categorizes "B-cell lymphoblastic leukaemias/lymphomas" into specific genetic entities. In our manuscript, the term "B-other" corresponds to the WHO category "B-lymphoblastic leukaemia/lymphoma with other defined genetic abnormalities," including cases with genetic alterations not assigned to specific categories.

For this study, MLPA, t-NGS, and OGM analyses were performed retrospectively following the standardized protocols (see Supplementary File). Karyotyping and FISH studies were performed on all patients, yielding evaluable results in 92% (n=161) and 92.6% (n=162) of cases, respectively. A retrospective t-NGS study included 84 patients, focusing particularly on the BCR::ABLI-like (n=16/17) and B-other (n=37/51) subtypes. Additionally, OGM study was performed on 11 undiagnosed patients with available cryopreserved material. MLPA analysis using the P335 kit (version C2) was conducted on 120 patients, while the P327 kit (version B2) was specifically applied to 26 B-other patients lacking a defined genetic subtype. For 12 patients, samples were unavailable for complete genetic diagnosis. All techniques performed for each patient are listed in Table S1.

The differences between groups were compared using the chi-square, Fisher's exact, and Mann–Whitney tests, as appropriate. P-values < 0.05 were considered statistically significant. Survival analysis focused on overall survival (OS), event-free survival (EFS), and relapse incidence were calculated using Kaplan–Meier methods. Materials,

procedures and statistical analyses are detailed in the Supplementary File.

This study was conducted in accordance with the Declaration of Helsinki.

Results

Evaluation of diagnostic techniques for B-ALL subtype classification

A total of 175 B-ALL patients with ALL were included in this study; the median age at diagnosis was 4 years (interquartile range [IQR] 3–10 years), the median white blood cell count was 11.18x10⁹/L (IQR 4.65–34.17), and there was a male predominance (57.7%). Five patients (2.9%) from the total cohort had Down Syndrome (DS) (Table S2).

Using all employed techniques, we were able to classify 145 out of 175 (83%) B-ALL patients into 17 distinct genetic subtypes (Table S1). Each technique demonstrated specific effectiveness for identifying particular genetic subtypes: karyotyping (39.1%), FISH (51.9%), t-NGS (59.5%), and OGM (54.5%) (Fig. 1A). Considering the most rapid and cost-effective approach, the combination of karyotyping and FISH allowed us to establish a diagnosis in 73% of cases. The addition of t-NGS and OGM further improved classification by an additional 10% (Fig. 1B).

Although not all cases were analyzed using every technique, it is noteworthy that some genetic entities could be diagnosed using multiple techniques in combination, while others were defined exclusively by a single method. For instance, in our series, aneuploidies were identified almost exclusively through karyotyping, IGH fusions solely by FISH, specific fusions and point mutations uniquely by t-NGS, and *NUTM1* rearrangements and *ERG* deletions only by OGM. Each technique had its limitations; for example, FISH missed certain cases, including P2RY8::CRLF2 (4/10), ZNF384 rearrangements (3/6), and KMT2A::AFF3 fusion (1/1), probably due to limitations in probe design and coverage. Additionally, t-NGS failed to detect IGH::CRLF2 (1/1), KMT2A::UPS2 (1/1), and a ZNF384 rearrangement (1/6). This underscores the added value of complementary approaches such as OGM, which is capable of identifying some of these alterations with greater precision.

Frequency and clinical significance of primary recurrent genetic in B-ALL

Among the 145 patients with a defined genetic diagnosis, 124 patients (71%) harbored a classical recurrent abnormality: high hyperdiploidy (HeH) (n = 46), t(12;21)/ETV6::RUNXI (n = 36), BCR::ABLI-like (n = 17), KMT2A rearrangements



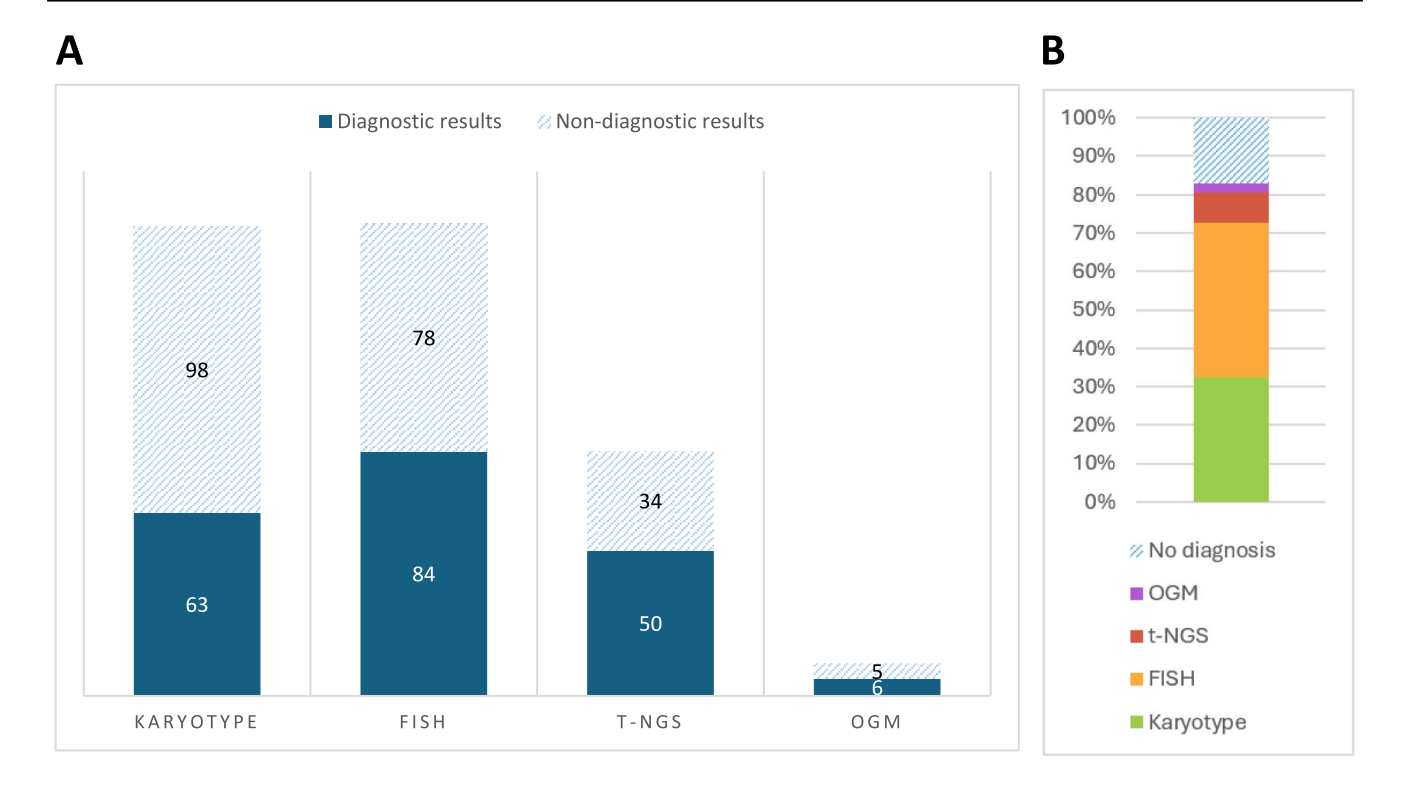


Fig. 1 Diagnostic performance of cytogenetic techniques in pediatric B-ALL diagnosis. (A) The bar chart illustrates the number of diagnostic and non-diagnostic results obtained using karyotyping, FISH, t-NGS, and OGM. (B) Proportion of patients classified into a defined genetic subtype using different cytoge-

netic techniques, ordered by increasing complexity (Karyotype < FISH < t-NGS < OGM). K: karyotype; FISH: fluorescence in situ hybridization; t-NGS: targeted next generation sequencing; OGM: optical genome mapping

(KMT2A-r) (n=8), t(1;19)/TCF3::PBX1 (n=6), t(9;22)/BCR::ABL1 (n=4), iAMP21 (n=4), and hypodiploidy (near haploidy (n=2) and low hypodiploidy (n=1)). The remaining patients were classified as B-other (29%) (Table 1, Fig. 2).

High hyperdiploidy (HeH) was the most prevalent genetic subtype, diagnosed primarily through karyotyping (39/46). FISH using specific probes (e.g., XCE 4/10/17 from Meta-Systems) was employed in patients without informative karyotype. The median number of chromosomes was 56 (IQR 55–60). Trisomies most frequently involved chromosomes X, 4, 10, 17, 18, and 21, rarely involving chromosomes 1, 13, 16, or 20. Additionally, 43.6% of cases had structural variants, most commonly a duplication in chromosome 1. Notably, HeH patients were typically younger (1–10 years old, p < 0.001) with lower WBC counts (p < 0.001) at diagnosis.

The second most prevalent genetic subtype was *ETV6::RUNX1* rearrangement, detected by FISH in all 36 patients and further confirmed by NGS when available. Among these patients, 75% presented an altered karyotype, with a median of 2 aberrations (IQR 1–5). Common accompanying alterations were trisomy 21 (36%) and deletion of 12p (33%). Of particular note, one case exhibited an atypical hyperdiploid characterized by the presence of an additional

chromosome 15, highlighting the importance of FISH, as without this test, the case could have been erroneously classified. Notably, patients with ETV6::RUNX1 were typically younger at diagnosis (1–10 years old, p = 0.005).

Seventeen patients (10%) harbored BCR::ABLI-like abnormalities, categorized as JAK-STAT abnormalities (7%) and ABL-class fusions (3%) (Table 2). JAK-STAT abnormalities included P2RY8::CRLF2 (n=10), IGH::CRLF2 (n=1), and PAX5::JAK2 (n=1). ABL-class fusions included PDGFRB-rearranged (n=3) and ABLI-rearranged (n=2). Partner genes were identified in three out of five cases (EBF1::PDGFRB, ETV6::ABLI, and NUP214::ABLI). Remarkably, patients with BCR::ABLI-like were typically older at diagnosis (p=0.033) and more likely to be male (p=0.03). Patients with CRLF2-rearranged were significantly associated with DS (60% (n=3) of patients with DS, p<0.001) and presented with higher WBC at diagnosis (p=0.018).

Eight patients harbored KMT2A-rearranged (KMT2A-r), with the partner gene identified in all cases: AFF1 (n = 3), MLLT3 (n = 3), AFF3 (n = 1), and USP2 (n = 1). Patients with KMT2A-r were diagnosed considerably at a younger age than the others, with 4/8 diagnosed within the first year of life (p < 0.001). This subtype also exhibited a high



Table 1 Demographic, Clinical, Genetic Features and Outcome of Patients with B-ALL according to genetic abnormalities

			,								
	Total cohort	Principal ge	Principal genetic subtype								
		НеН	ETV6::RUNXI	KMT2A-r	TCF3::PBX1 BCR::ABL1		iAMP21	Hypodiploid	<i>BCR::ABLI-</i> Like	B-other	<i>p</i> -value
	N (%)	N (%)	N(%)	N (%)	N (%)	N (%)	N(%)	N (%)	N (%)	N (%)	
	175	46 (26)	36 (21)	8 (5)	6 (3)	4 (2)	4 (2)	3 (2)	17 (10)	51 (29)	
Demographics features	ics features										
Sex											
Male	101 (58)	22 (48)	23 (64)	4 (50)	4 (67)	3 (75)	3 (75)	1 (33)	14 (82)	27 (53)	0.325
Female	74 (42)	24 (52)	13 (36)	4 (50)	2 (33)	1 (25)	1 (25)	2 (67)	3 (18)	24 (47)	
Age											
< 10	128 (73)	45 (98)	33 (92)	7 (88)	3 (50)	1 (25)	2 (50)	2 (67)	8 (47)	27 (53)	0.000
> 10	47 (27)	1 (2)	3 (8)	1 (12)	3 (50)	3 (75)	2 (50)	1 (33)	9 (53)	24 (47)	
White cell c	White cell count $(\times 10^9/L)$										
$< 20 \times 10^{9} / L$. 110 (65)	36 (82)	26 (72)	1 (12)	4 (67)	2 (50)	4 (100)	2 (67)	7 (44)	28 (58)	0.004
$\geq 20 \times 10^{9} \text{/L}$. 59 (35)	8 (18)	10 (28)	7 (88)	2 (33)	2 (50)	0 (0)	1 (33)	9 (56)	20 (42)	
Immunopheno-	-ou										
type											
Pro B	8 (4)	0 (0)	0 (0)	5 (63)	0 (0)	0 (0)	0 (0)	0 (0)	0 (0)	3 (6)	0.000
Common B	151 (87)	44 (96)	34 (94)	0 (0)	5 (83)	3 (75)	4 (100)	3 (100)	15 (88)	43 (86)	
Pre B	12 (7)	2 (4)	2 (6)	0 (0)	1 (17)	1 (25)	0 (0)	0 (0)	2 (12)	4 (8)	
Mature B	3 (2)	0 (0)	0 (0)	3 (37)	0 (0)	0 (0)	0 (0)	0 (0)	0 (0)	0 (0)	
Outcomes											
MDR status (+15 days)	(+15 days)										
Negative (< 0, 39 (24) 1%)	< 0, 39 (24)	13 (29)	9 (26)	2 (33)	2 (40)	0 (0)	0 (0)	0 (0)	1 (8)	12 (25)	0.557
Positive (\geq 0 1%)	Positive (≥ 0 , 121 (76) 1%)	31 (71)	26 (74)	4 (67)	3 (60)	3 (100)	4 (100)	3 (100)	12 (92)	35 (75)	
MDR status	MDR status (+33 days)										
Negative (<1%)	155 (95)	43 (98)	34 (100)	6 (100)	6 (100)	3 (100)	4 (100)	2 (67)	13 (93)	44 (90)	0.166
Positive $(\geq 1\%)$	8 (5)	1 (2)	0 (0)	0 (0)	0 (0)	0 (0)	0 (0)	1 (33)	1 (7)	5 (10)	
Complete remission	mission										
No	7 (4)	0 (0)	0 (0)	0 (0)	0 (0)	1 (33)	0 (0)	0 (0)	2 (12)	4 (8)	0.145
Yes	164 (96)	45 (100)	35 (100)	8 (100)	6 (100)	2 (67)	4 (100)	3 (100)	14 (88)	47 (92)	ļ
Relapse											



 Table 1 (continued)

Tota	Total cohort	Principal genetic subtype	netic subtype								
		нен	ETV6::RUNXI	KMT2A-r	TCF3::PBX1 BCR::ABL1	BCR::ABL1	iAMP21	Hypodiploid	BCR::ABLI- Like	B-other	p-value
N (%)	(%)	N (%)	N(%)	N (%)	N (%)	N (%)	N(%)	N (%)	N (%)	N(%)	
No 135	135 (78)	41 (91)	30 (86)	3 (38)	4 (67)	4 (100)	3 (75)	2 (67)	8 (47)	40 (80)	0.001
	37 (22)	4 (9)	5 (14)	5 (62)	2 (33)	(0) 0	1 (25)	1 (33)	9 (53)	10 (20)	
II.	ő		Í	Í				ĺ	į	9	
	154 (88)	46 (100)	35 (97)	3 (37)	5 (83)	2 (50)	4 (100)	2 (67)	12 (71)	45 (88)	0.000
Yes 21 (21 (12)	0 (0)	1 (3)	5 (63)	1 (17)	2 (50)	0 (0)	1 (33)	5 (29)	6 (12)	
Outcome rates at 5 years *	years *										
Relapse (%) 17.40%	40%	3.00%	4.40%	50.00%	No relapse	1	25.00%	33.30%	73.50%	28.00%	
Event free (%) 78.90 %	%06	%00.76	92.50%	50.00%	No events	1	75.00%	%01.99	26.50%	%08.99	
Overall sur- 88.9 vival (%)	88.90%	No death	%01.96	50.00%	No deaths	ı	No death	20.00%	51.10%	87.80%	
Genetic characteristics	tics										
Concurrent		1	2 P2RY8::CRLF2 -	2 -	1 Hyperdip-	2 Hyperdip-	2 P2RY8::CRLF2 -	72 -	∇	∇	
primary alterations			1 Hyperdiploidy		loidy	loidy					
Secondary alterations (CNA)	ins (CNA)										
EBFI deletion 8 $(N;\%)$		1 (12)	3 (38)	0 (0)	0 (0)	0 (0)	1	1 (12)	1 (13)	2 (25)	0.027
IKZFI dele- 21 tion $(N;\%)$		2 (9)	1 (5)	1 (5)	0 (0)	0 (0)	1	1 (5)	9 (43)	7 (33)	0.000
JAK2 deletion 9 $(N;\%)$		0 (0)	2 (22)	(0) 0	1 (11)	0 (0)	1	1 (11)	2 (22)	3 (34)	0.087
CDKN2A/B 30 deletion (N;%)		4 (14)	6 (20)	1 (3)	1 (3)	1(3)	1	1 (3)	7 (24)	9 (30)	0.100
<i>PAX5</i> deletion 26 $(N;\%)$		0 (0)	7 (27)	0 (0)	1 (4)	0 (0)	1	1 (4)	6 (23)	11 (42)	0.004
ETV6 deletion 31 $(N;\%)$		7 (23)	13 (42)	(0) 0	1 (3)	0 (0)	1	1 (3)	3 (10)	6 (19)	0.035
BTGI deletion 9 (N;%)		1 (11)	4 (45)	(0) 0	0 (0)	0 (0)	1	1 (11)	3 (33)	0 (0)	0.003
RBI deletion 11 $(N;\%)$		0 (0)	2 (18)	1 (9)	0 (0)	1 (9)	1	1 (9)	0 (0)	7 (64)	0.001
<i>PAR1</i> deletion 6 (<i>N</i> ;%)		0 (0)	3 (50)	0 (0)	0 (0)	0 (0)	1	0 (0)	3 (50)	0 (0)	0.000

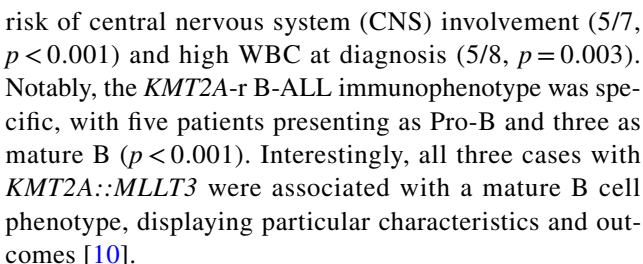


(continued)
_
e
虿
ā

	Total cohort	Total cohort Principal genetic subtype	netic subtype								
		нен	ETV6::RUNXI KMT2A-r TCF3::PBXI BCR::ABLI iAMP21	KMT2A-r	TCF3:::PBX1	BCR::ABL1	iAMP21	Hypodiploid	Hypodiploid $BCR::ABLI$ - B-other p -value Like	B-other	<i>p</i> -value
	N(%)	N(%)	N(%)	N (%)	N(%) $N(%)$ $N(%)$	N (%)	N(%)	N (%)	N (%)	N (%)	
Median number of deletions	.	0	1	0	0.5	1		∞	2	-	
Median number of mutations		8		2		0	0	2.5	1.5	2	

*Only patients treated homogeneously with the SEHOP-PETHEMA 2013 protocol (144/175) Δ See Table 2

NA, not applicable



TCF3::PBX1 (n=6), BCR::ABL1 (n=4), and iAMP21 (n=4) were detected. TCF3::PBX1 and BCR::ABL1 displayed unbalanced translocations [der(19)t(1;19) or der(22) t(9;22)] in 4/6 and 1/4 of cases, respectively. Remarkably, patients with TCF3::PBX1 harbored complex karyotypes with at least three karyotypic alterations (p=0.029). None of the cases with KMT2A-r, TCF3::PBX1, BCR::ABL1, or hypodiploidy displayed any additional recurrent alterations (Table 1).

B-other Subtype: Genetic and Clinical Features

Any recurrent genetic abnormality was observed in 51 patients (29%), comprising the B-other subtype. Particularly, B-other patients were diagnosed at a significantly older age compared to the entire B-ALL cohort (p < 0.001), with nearly half (47%) being diagnosed after age 10. This subgroup also had a significantly higher MRD positivity rate (p = 0.04), accounting for 62.5% of all MRD-positive cases within the study cohort (Table 2).

A specific genetic subtype was identified in 21 patients (Fig. 2). Six patients (12% of B-other) harbored ZNF384 rearrangements (ZNF384-r), with partner genes identified in most cases: $EP300 \ (n=2)$ and $TCF3 \ (n=3)$. Four patients (8%) displayed PAX5 alterations (PAX5alt), concretely two harbored PAX5 rearrangements and two presented a unique clonal PAX5 mutation. Three patients (6%) displayed the defining PAX5 P80R mutation and another three presented IGH rearrangements (IGH-r). Notably, both PAX5 P80R and IGH-r patients were typically diagnosed at an older age (> 10 years old, p = 0.016) compared to the entire B-ALL cohort. Additionally, patients with IGH-r exhibited a higher prevalence of CNS involvement (p = 0.001). ERG deletions were identified in three patients (6%), being classified as DUX4 rearrangements since the intragenic ERG deletion are found exclusively in those cases [11, 12]. Finally, one case with NUTM1 rearrangement (2%) and another case with the IKZF1 N159Y mutation (2%) were identified. Interestingly, the IKZF1 mutation was observed in the Pre-B ALL phenotype (p = 0.004).



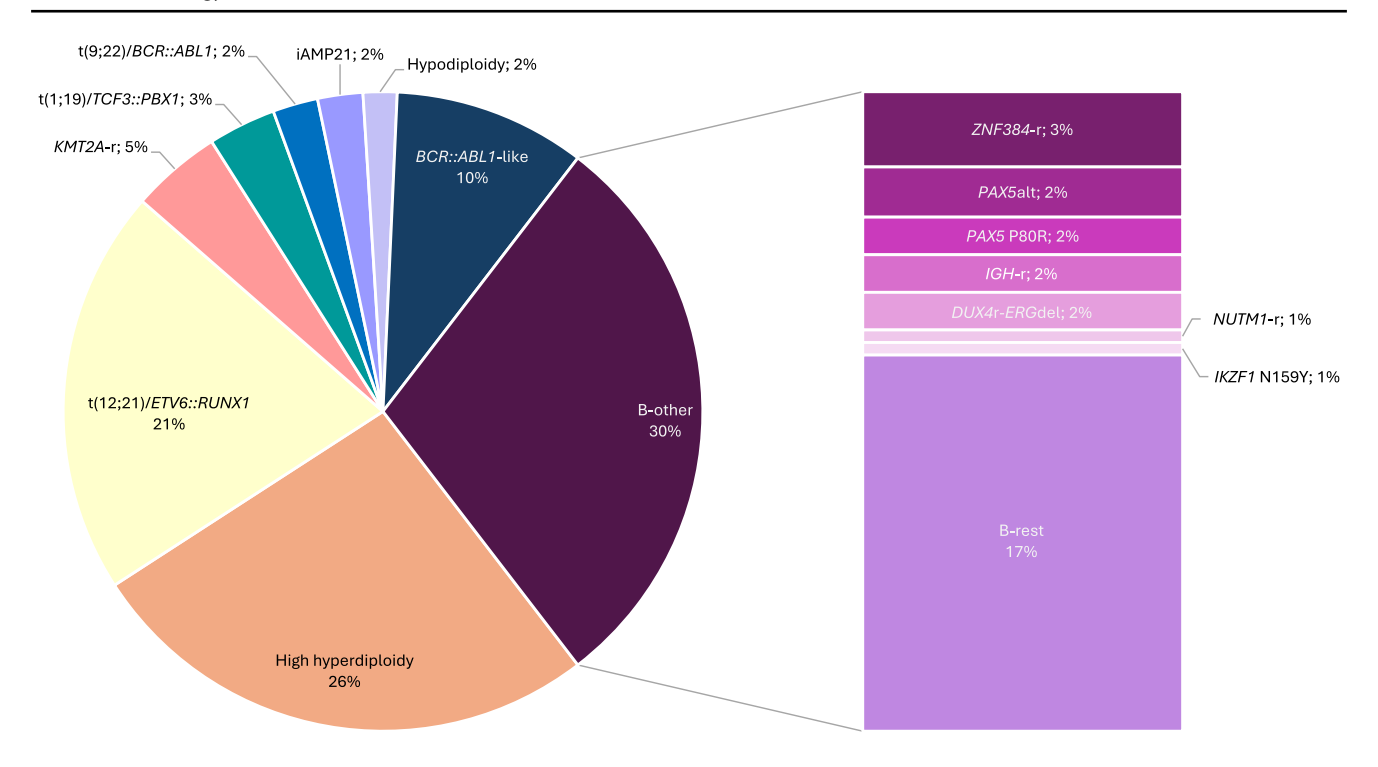


Fig. 2 Genetic distribution of 175 pediatric B-ALL patients in our series. Pie chart segments display the proportion of patients within each genetic subtype. The B-other group is further subdivided based

on the specific identified subtypes. alt: alterations; r: rearrangements; del: deletion

Frequency of copy number alterations in correlation with primary chromosomal abnormalities

Copy number alterations (CNAs) affecting IKZF1, CDKN2A/B, PAX5, BTG1, ETV6, EBF1, RB1, and the PAR1 region were determined by P335 MLPA in 120 patients. No detectable CNVs were observed in 26% of the patients. The median number of deletions in the cohort was 1. Among patients with deletions, 73 (60%) had one or more deletions, with 26%, 17%, and 18% exhibiting 1, 2, or ≥ 3 deletions, respectively. The most frequently deleted genes were ETV6 (26%), CDKN2A/B (25%), PAX5 (22%), and IKZF1 (18%). Deletions in other investigated genes (BTG1, EBF1, RB1, and PAR1) were observed in less than 10% of patients. Among patients with IKZF1 deletions, the most frequent type involved canonical intragenic deletions encompassing exons 4-7 (42%). Notably, 53% of patients with CDKN2A/B deletions exhibited biallelic loss, a phenomenon observed only in this particular gene pair. Pairwise testing revealed a non-random pattern in CNAs (Figure S1). IKZF1 deletions frequently co-existed with PAR1 deletions (p = 0.009). CDKN2A/B, and PAX5, which are co-located on chromosome 9p, were also frequently co-deleted (p < 0.001).

According to the classification proposed by Hamadeh et al. [13], CNA profiles could be categorized as good-risk (CNA-GR; n=69) or poor-risk (CNA-PR; n=51). CNA-GR

included cases with no deletions in any of the regions studied, isolated deletions of ETV6, PAX5, or BTG1, or deletions of ETV6 combined with single deletions of BTG1, CDKN1A/B, or PAX5. Conversely, CNA-PR comprised any deletion of IKZF1, PAR1, EBF1, RB1, or any other CNAprofile not mentioned above. The deletion pattern varied significantly depending on the underlying primary chromosomal abnormality (Fig. 3). HeH patients frequently presented a CNA-GR (p < 0.001). ETV6::RUNX1 cases presented the majority of ETV6 deletions (representing the 65% of all ETV6 deletions; p < 0.001). Deletions were detected in all BCR::ABL1-like cases (median 2), associated with a CNA-PR in the majority of cases (p < 0.001). The most common deletions in this subtype were *IKZF1* (75%), CDKN2A/B (58%) and PAX5 (50%). IKZF1 and PAR1 region were significantly deleted in BCR::ABL1-like patients compared to overall B-ALL (p < 0.001). All patients with CRLF2-r exhibited deletions (median 2.5), frequently in IKZF1, CDKN2A/B, PAX5, and PAR1 (p < 0.01). KMT2A-r or TCF3::PBX1 subtypes were not associated with any specific deletions, and most patients had a normal CNA profile.

The B-other subgroup displayed a higher frequency of deletions (52.8%), with a median of 1 deletion. Most patients presented deletion of *PAX5* (30.6%), *CDKN2A/B* (25%), *IKZF1* and *RB1* (19.4% both). Patients with *PAX5*alt and *ZNF384*-r consistently presented with multiple deletions (median 3 and 2.5, respectively). Additionally, all patients



Table 2 Demographic, Clinical, Genetic Features and Outcome of Patients with B-other and BCR::ABLI-like subtypes

	Total	B-OTHER subtypes	ubtypes							Total	BCR::ABL1-LIKE subtypes	btypes		
	B-OTHER	ZNF384-r	PAX5alt	PAX5 P80R	IGH-r	DUX4- ERGdel	NUTM1-r	IKZF1 NI 59Y	B-rest	<i>BCK::ABLI-</i> LIKE	CRLF2-r	PDGFRB-r	ABL1-r	JAK2-r
	N(%)	N(%)	N(%)	N(%)	N(%)	N(%)	N(%)	N(%)	N(%)	N(%)	N(%)	N(%)	N(%)	N(%)
Total	51	6 (12)	4 (8)	3 (6)	3 (6)	3 (6)	1 (2)	1 (2)	30 (58)	17	11 (65)	3 (17)	2 (12)	1 (6)
Demographics features														
Sex														
Male	27 (53)	2 (33)	4 (100)	3 (100)	3 (100)	1 (33)	1 (100)	1 (100)	12 (40)	14 (82)	2 (18)	3 (100)	1 (50)	1 (100)
Female	24 (47)	4 (67)	0 (0)	0 (0)	0 (0)	2 (67)	0 (0)	0 (0)	18 (60)	3 (18)	9 (82)	0 (0)	1 (50)	0 (0)
Age														
<10	27 (53)	4 (67)	2 (50)	0 (0)	0 (0)	1 (33)	<u> </u>	1 (100)	18 (60)	8 (47)	7 (64)	1 (33)	0 (0)	0 (0)
≥10	24 (47)	2 (33)	2 (50)	3 (100)	3 (100)	2 (67)	0 (0)	0 (0)	12 (40)	9 (53)	4 (36)	2 (67)	2 (100)	1 (100)
White cell count $(x10^9/L)$														
$<20x10^{9}/L$	28 (58)	1 (17)	2 (50)	3 (100)	3 (100)	2 (67)	1 (100)	1 (100)	15 (56)	7 (44)	4 (40)	1 (33)	2 (100)	0 (0)
≥20x10 ⁹ /L	20 (42)	5 (83)	2 (50)	0 (0)	0 (0)	1 (33)	0 (0)	0 (0)	12 (44)	6 (56)	(09) 9	2 (67)	0 (0)	1 (100)
Immunophe- notype														
Pro B	3 (6)	1 (17)	0 (0)	1 (33)	0 (0)	0 (0)	0 (0)	0 (0)	1 (3)	0 (0)	0 (0)	0 (0)	0 (0)	0 (0)
Common B	43 (86)	5 (83)	4 (100)	2 (67)	3 (100)	2 (67)	1 (100)	0 (0)	26 (90)	15 (88)	10 (91)	3 (100)	1 (50)	1 (100)
Pre B	4 (8)	0 (0)	0 (0)	(0) 0	0 (0)	1 (33)	0 (0)	1 (100)	2 (7)	2 (12)	1 (9)	0 (0)	1 (50)	0 (0)
Mature B	0 (0)	0 (0)	0 (0)	0 (0)	0 (0)	0 (0)	0 (0)	0 (0)	0 (0)	0 (0)	0 (0)	0 (0)	0 (0)	0 (0)
Outcomes														
MDR status (+15 days)														
Negative (<0,1%)	12 (25)	0 (0)	2 (67)	1 (33)	0 (0)	0 (0)	1 (100)	1 (100)	7 (26)	1 (8)	0) (0)	0 (0)	1 (50)	0 (0)
Positive $(\geq 0, 1\%)$	35 (75)	6 (100)	1 (33)	2 (67)	3 (100)	3 (100)	0 (0)	0 (0)	20 (74)	12 (92)	8 (100)	3 (100)	1 (50)	1 (100)
MDR status (+33 days)														
Negative (<1%)	44 (90)	5 (83)	3 (100)	3 (100)	3 (100)	3 (100)	1 (100)	1 (100)	25 (86)	13 (93)	9 (100)	3 (100)	1 (50)	0) 0
Positive (≥1%)	5 (10)	1 (17)	0 (0)	0 (0)	0 (0)	0 (0)	0 (0)	0 (0)	4 (14)	1 (7)	0 (0)	0 (0)	1 (50)	1 (100)
Complete remission														
No	4 (8)	0 (0)	1 (25)	0 (0)	1 (33)	0 (0)	0 (0)	0 (0)	2 (7)	2 (12)	1 (9)	1 (33)	0 (0)	1(100)
Yes	47 (92)	6 (100)	3 (75)	3 (100)	2 (67)	3 (100)	1 (100)	1 (100)	29 (93)	14 (88)	10 (91)	2 (67)	2 (100)	0 (0)
Relapse														
o _N	40 (80)	6 (100)	3 (75)	3 (100)		3 (100)	<u> </u>	0 (0)	22 (76)	8 (47)	4 (36)	2 (67)	<u>(</u>	0 (0)
Yes	10 (20)	0 (0)	1 (25)	(0) 0	1 (33)	0 (0)	0 (0)	1 (100)	7 (24)	9 (53)	7 (64)	1 (33)	0 (0)	1 (100)



Table 2 (continued)

iable 2 (co	(commuca)													
	Total	B-OTHER subtypes	ubtypes							Total	BCR::ABL1-LIKE subtypes	otypes		
	B-OTHER	ZNF384-r	PAX5alt	PAX5 P80R	IGH-r	DUX4- ERGdel	NUTM1-r	IKZF1 N159Y	B-rest	BCK::ABLI- LIKE	CRLF2-r	PDGFRB-r	ABLI-r	JAK2-r
	N(%)	N(%)	N(%)	N(%)	N(%)	N(%)	N(%)	N(%)	N(%)	N(%)	N(%)	N(%)	N(%)	N(%)
Death														
No	45 (88)	5 (83)	3 (75)	3 (100)	3 (100)	2 (67)	1 (100)	1 (100)	27 (90)	12 (71)	7 (64)	2 (67)	2 (100)	1 (100)
Yes	6 (12)	1 (17)	1 (25)	0 (0)	0 (0)	1 (33)	0 (0)	0 (0)	3 (10)	5 (29)	4 (36)	1 (33)	0 (0)	0 (0)
Outcome rates at 5 years *	at 5 years *													
Relapse rate	28.00%	No relapse	33.30%	No relapse	*	*	*	* *	34.10%	73.50%	72.70%	*	*	* *
Event free	%08.99	83.30%	50.00%	No events	* *	*	*	* *	65.90%	26.50%	27.30%	*	*	* *
Overall survival	87.80%	83.30%	75.00%	No death	*	* *	*	* *	%06.06	51.10%	52.50%	* *	*	* *
Genetic characteristics	teristics													
Concurrent pri	Concurrent primary alterations 1 IGH-r	1 <i>IGH</i> -r				1 <i>IGH</i> -r		,			1 MYH9::IL2RB	1 P2RY8::CRLF2	1 P2RY8::CRLF2	
Secondary alte	Secondary alterations (CNA)													
EBFI deletion $(N;\%)$	2	2 (100)	0 (0)	0 (0)	0 (0)	0 (0)	0 (0)	0 (0)	0 (0)	_	0 (0)	1 (100)	0) 0	0 (0)
IKZFI deletion (N;%)	7	3 (43)	1 (14)	0 (0)	0 (0)	0 (0)	0 (0)	0 (0)	3 (43)	6	(6 (67)	1 (11)	1 (11)	1 (11)
JAK2 deletion (N;%)	1 3	0 (0)	2 (67)	1 (33)	0 (0)	0 (0)	0 (0)	0 (0)	0 (0)	7	1 (50)	0 (0)	1 (50)	0 (0)
CDKN2A/B deletion (N;%)	6	0 (0)	3 (33)	1 (11)	0 (0)	2 (23)	0 (0)	0 (0)	3 (33)	7	5 (71)	0 (0)	2 (29)	(0) 0
PAX5 deletion (N;%)	11	1 (9)	3 (27)	1 (9)	0 (0)	1 (9)	0 (0)	0 (0)	5 (46)	9	5 (83)	0 (0)	1 (17)	0 (0)
ETV6 deletion (N;%)	9	4 (66)	0 (0)	(0) 0	1 (17)	1 (17)	0 (0)	0 (0)	(0) 0	3	2 (67)	0 (0)	1 (33)	(0) 0
BTG1 deletion (N;%)	0	0 (0)	0 (0)	0 (0)	0 (0)	0 (0)	0 (0)	0 (0)	0 (0)	3	2 (67)	0 (0)	0 (0)	1 (33)
RB1 deletion (N;%)	7	2 (29)	1 (14)	0 (0)	1 (14)	0 (0)	0 (0)	0 (0)	3 (43)	0	0 (0)	0 (0)	0 (0)	0 (0)
PARI deletion (N;%)	0	0 (0)	0 (0)	(0) 0	(0) 0	(0) 0	0 (0)	0 (0)	(0) 0	3	3 (100)	0 (0)	0 (0)	(0) 0
Median number of deletions	1	2.5	ю	1.5	0	2	0	0	0	2	2.5	2	ы	2
Median number of mutations	7	2	3.5	2	1	8	0	7	-	1.5	2.5	1	ъ	0
* Only patient	* Only natients treated homogeneously with the SEHOP-PETHEMA 2013	eously with t	he SEHOP-1	PETHEMA 20)13									

 \ast Only patients treated homogeneously with the SEHOP-PETHEMA 2013 protocol.

 $[\]ast\ast\ast$ Outcome rates could not be estimated because a 5-year follow-up was not reached.



	Total	B-OTHER subtypes	abtypes							Total	BCR::ABLI-LIKE subtypes	abtypes		
	B-OTHER	ZNF384-r PAX5alt	PAX5alt	PAX5 P80R	IGH-r	DUX4- ERGdel	NUTM1-r	IKZF1 NI 59Y	B-rest	LIKE	CRLF2-r	PDGFRB-r	ABLI-r	JAK2-r
	N(%)	N(%)	N(%)	N(%)	N(%)	N(%)	N(%)	N(%)	N(%)	N(%)	N(%)	N(%)	N(%)	N(%)
NA: not appli-														

with *PAX5* alt had deletions in *CDKN2A/B* and *PAX5* itself (p < 0.01), and deletions of *EBF1* and *RB1* were more frequent in patients with *ZNF384*-r compared to the overall cohort (p < 0.05).

Frequency of mutations in correlation with primary chromosomal abnormalities

Pathogenic mutations were identified in 70.6% of patients. The most frequently mutated genes were *KRAS* (23.8%), *NRAS* (15.5%), and *PAX5* (8.3%). These were followed by mutations in *TP53*, *FLT3*, *NF1*, *PTPN11*, and *KMT2D* (around 6%). Mutations in *IKZF1*, *JAK1*, *NSD2*, *CBL*, and *ARID1A* (around 4.8%) were also observed, along with less frequent mutations (1–2.5%) in 22 other genes. Overall, the median number of mutations per patient was 1.5 (IQR 0–3 mutations).

The specific chromosomal abnormalities of a patient significantly influenced their mutation profile (Fig. 4). Patients with HeH displayed a high number of mutations (median 3) and frequently harbored concurrent mutations in NT5C2, FLT3, and PTPN11. ETV6::RUNX1 cases often had mutations in KRAS, ARID1A, and KMT2D. The BCR::ABL1-like patients had the highest overall mutation frequency (63%), with mutations commonly involving KRAS, NRAS, CBL, JAK1, and JAK2. Notably, all JAK2 mutations occurred in patients with CRLF2-r.

In the B-other subtype, KRAS and NRAS mutations were highly prevalent, accounting for 70% and 62% of the total mutated gene, respectively. Similarly, PAX5 and IKZF1 mutations were also common (71.4% and 75% of mutations, respectively). Furthermore, co-occurring mutations in TP53, FLT3, NF1, CBL, NSD2, JAK1, and PTPN11 were frequently observed within this subtype. The PAX5alt group displayed the highest number of mutations (median 3.5), with all PAX5 mutations co-occurring with MTOR mutations. Furthermore, the PAX5 P80R specific mutation frequently co-occurred with other mutations (median 2). Patients with ZNF834-r harbored all the mutations found in EGFR and EZH2 genes.

It is important to note that mutations with high variant allele frequency (VAF > 40%) were observed in several cases, particularly in TP53. These cases warrant special attention during remission to determine whether the mutations are somatic or germline. This distinction is crucial for clinical decisions regarding allogeneic transplantation, especially when considering family donors, as well as for genetic counseling in cases of constitutional TP53 mutations [14].



Table 2 (continued)

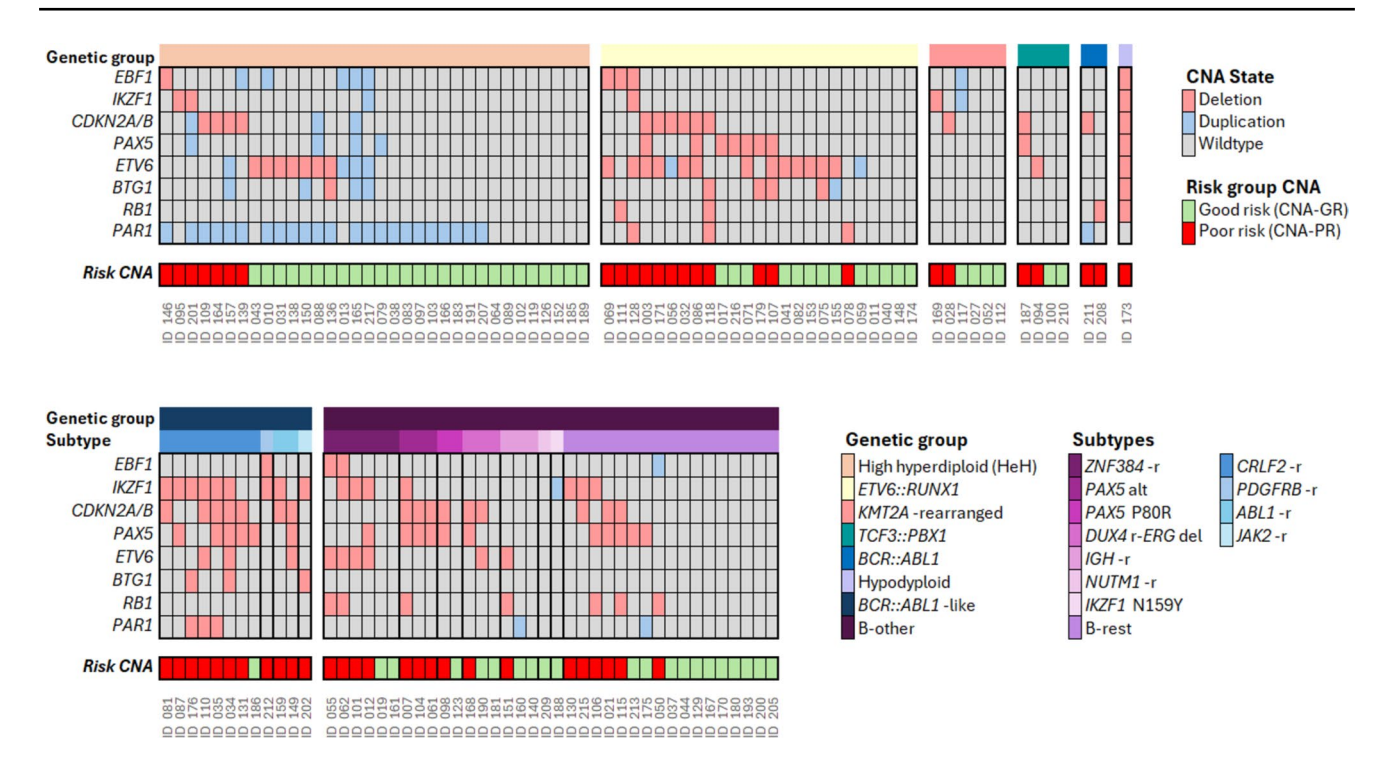


Fig. 3 Copy number alteration (CNA) pattern across the underlying genetic subtype in our cohort of B-ALL. Oncoplot showing the pattern of individual copy number alterations, deletions (red) and duplication (blue), and the risk group profile of CNA per case according to genetic subtype. Risk groups were established based on UKALL-CNA profile established by Hamadeh et al. [13]. CNA-GR

(green): do not present any deletion of the regions studied, isolated deletions of *ETV6*, *PAX5* or *BTG1*, or cases with *ETV6* deletions with single additional deletion of *BTG1*, *PAX5* or *CDKN2A/B*; CNA-PR (red): any deletion of *IKZF1*, *PAR1*, *EBF1*, *RB1*, or any other CNA-profile not mentioned above

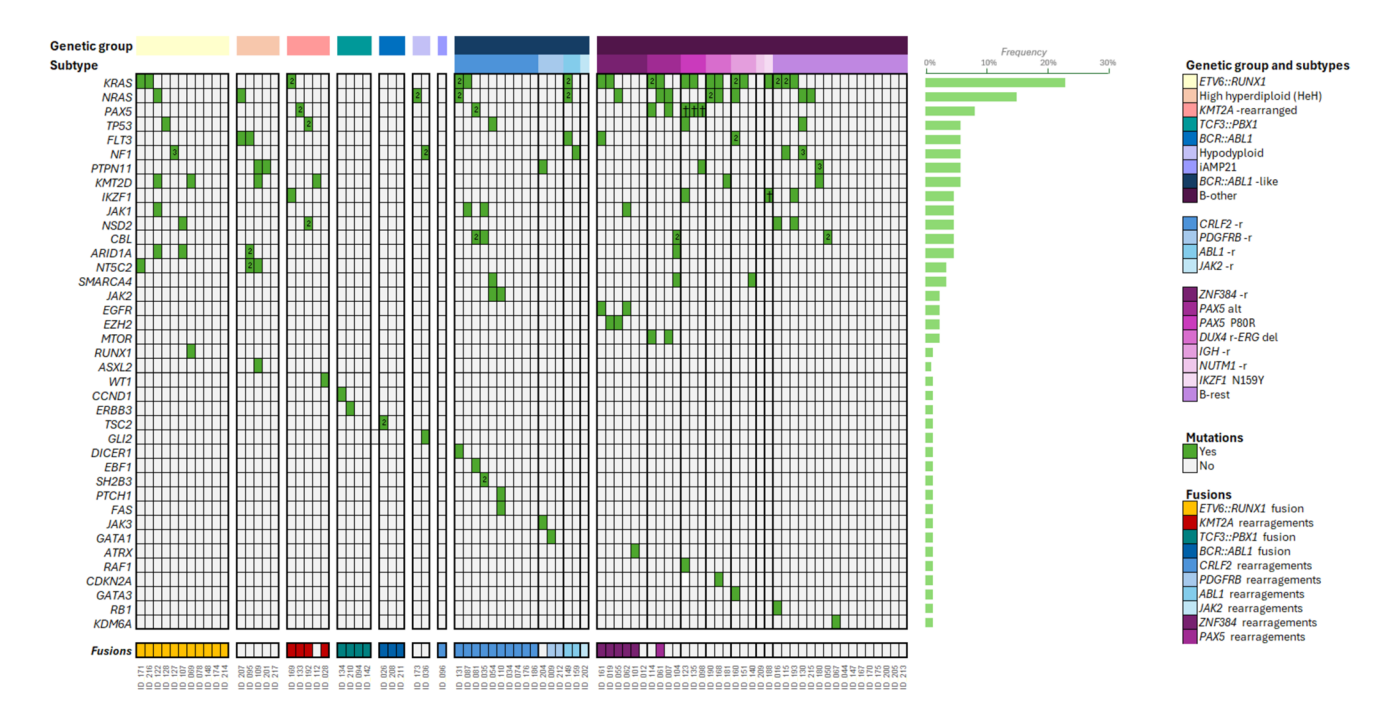


Fig. 4 Distribution of Mutations and Fusions Across B-ALL Subtypes. The oncoplot displays mutations (in green) and fusions (color-coded in the legend) for each patient in our B-ALL cohort, organized by genetic subtype. For genes with multiple mutations in a single

sample, the number indicates the total mutations in that gene. The mutation frequency for each gene is also shown. Mutations marked with † are defining for specific genetic subtypes, such as *PAX5* P80R and *IKZF1* N159Y



Outcome of patients by genetic subtype and prognostic impact of secondary abnormalities

A total of 144 B-ALL patients in this study were treated according to the SEHOP-PETHEMA 2013 treatment guidelines, which use risk-adapted treatment regimens (see supplementary data). Patients were classified as standard (n=5), intermediate (n=98), or high-risk (n=41). The 5-years overall survival (OS) rates were 100%, 97.0%, and 68.6% respectively; and event-free survival (EFS) rates were 75%, 89.6%, and 54.1% (Figure S2). The entire B-ALL cohort showed high OS and EFS rates of 88.9% and 78.9%, respectively, with a relapse rate of 17.4% (Table 1).

Distinct genetic subtypes of B-ALL patients exhibited distinct survival and relapse rates (Table 1, Figure S3). HeH patients had a significantly lower relapse rate (only 9%, p = 0.016) and all are currently alive (p = 0.004). In contrast, BCR::ABL1-like patients displayed a high relapse rate (53%, p = 0.001) and mortality rate (29%, p = 0.02); specifically, the CRLF2-r subgroup showing poorer outcomes, with a significantly higher relapse rate (63%, p < 0.001) and mortality rate (36%, p = 0.01). Similarly, KMT2A-r patients also had high relapse rate (63%, p = 0.004) and mortality rate, with all relapses in this group resulting in death (p < 0.001). Therefore, BCR::ABL1-like and KMT2A-r, along with hypodiploid and BCR::ABL1 patients, exhibited the worst outcomes. B-other patients demonstrated an intermediate-risk profile, with a 5-years OS of 87.8% and an EFS of 66.8% (Table 2). Interestingly, among the B-other subgroup, ZNF384-r and PAX5 P80R patients exhibited the lowest mortality and relapse rates. These prognostic findings should be interpreted with caution, as they are based on data from a single-center study with a relatively small cohort in certain subgroups, potentially limiting the statistical power of some observations.

Based on cytogenetic prognosis profiles, we classified patients into three distinct risk groups: good (CYTO-GR, n = 73, characterized by HeH and ETV6::RUNX1), poor (CYTO-PR, n=7, with KMT2A-r, BCR::ABL1 and hypodiploidy), and intermediate (CYTO-IR, n = 64, encompassing other genetic subtypes). CYTO-GR, CYTO-IR, and CYTO-PR presented at 5-years an OS rates of 98.5%, 83.0%, and 38.1%; an EFS of 94.9%, 64.1%, and 42.9%; and a relapse incidence of 3.7%, 32.7%, and 37.5%, respectively (Fig. 5). Despite differences in survival rates between genetic risk groups, CYTO-IR and CYTO-PR patients exhibited similar relapse rates. Furthermore, incorporating CNAs data with these genetic groups did not significantly affect patient prognosis in our study (Figure S4). In the overall series, the presence of a complex karyotype also showed no impact on survival outcomes (Figure S5).

Discussion

With our comprehensive approach, which combines karyotyping, FISH, t-NGS, and OGM, we classified 83% of patients into 17 distinct genetic subtypes. Despite this, 58% of B-other cases (17% of all B-ALL) in our study remained unclassified—a result broadly consistent with other large studies, such as Schwab et al. [15], where even with WGS, 53% of cases were unclassified.

Based on our experience and the classification rates achieved by each technique in our study, we propose a diagnostic workflow algorithm for the genetic characterization of B-ALL. This algorithm begins with karyotyping and FISH screening for ETV6::RUNX1, KMT2A, TCF3, and ABL-class genes (ABL1, ABL2, PDGFRB, and CSF1R), enabling us to achieve a genetic diagnosis in 63.4% of cases. If these techniques do not yield a definitive diagnosis, an extended FISH panel with probes for CRLF2, EPOR, JAK2, PAX5, MEF2D, and ZNF384 is performed, allowing us to diagnose an additional 9.1% of cases. In parallel, targeted NGS (t-NGS) is applied, providing diagnoses in a further 8% of cases. For cases that remain undiagnosed and with available material, OGM is used as a final step, identifying an additional 2.3% of cases (Fig. 6). This approach enables us to reach a diagnosis in 63.4% of cases with only the initial step, minimizing the need for further testing for the majority of patients. Similar workflows have been described in the literature, such as the guidelines proposed by Tueur et al. [16], which emphasize the integration of cytogenetic and advanced molecular techniques for comprehensive characterization of B-ALL. Therefore, karyotyping and FISH remain effective, rapid, cost-efficient, and accessible tools for detecting chromosomal abnormalities, while t-NGS significantly enhances diagnostic yield, particularly in cases with incomplete cytogenetic results. Further research is necessary to evaluate the potential of early OGM implementation in B-ALL diagnostics, considering factors such as turnaround time and cost.

The distribution of most identified genetic subtypes aligned well with previous studies [17, 18]. However, *DUX4*-r, *ZNF384*-r, and *PAX5*alt, were observed at a lower frequency in our study compared to the reported range (2%vs4-7%, 3%vs6%, and 2%vs10%, respectively) [15, 17–19]. No cases of *MEF2D* rearrangements were identified despite using techniques with sufficient coverage. This difference in frequency and identification of the subtypes could be due to variations in the studied populations, as geographic location or ethnicity might influence the prevalence of certain subtypes. Importantly, we identified patients with potential *DUX4*-r based solely on *ERG* deletions. Currently,



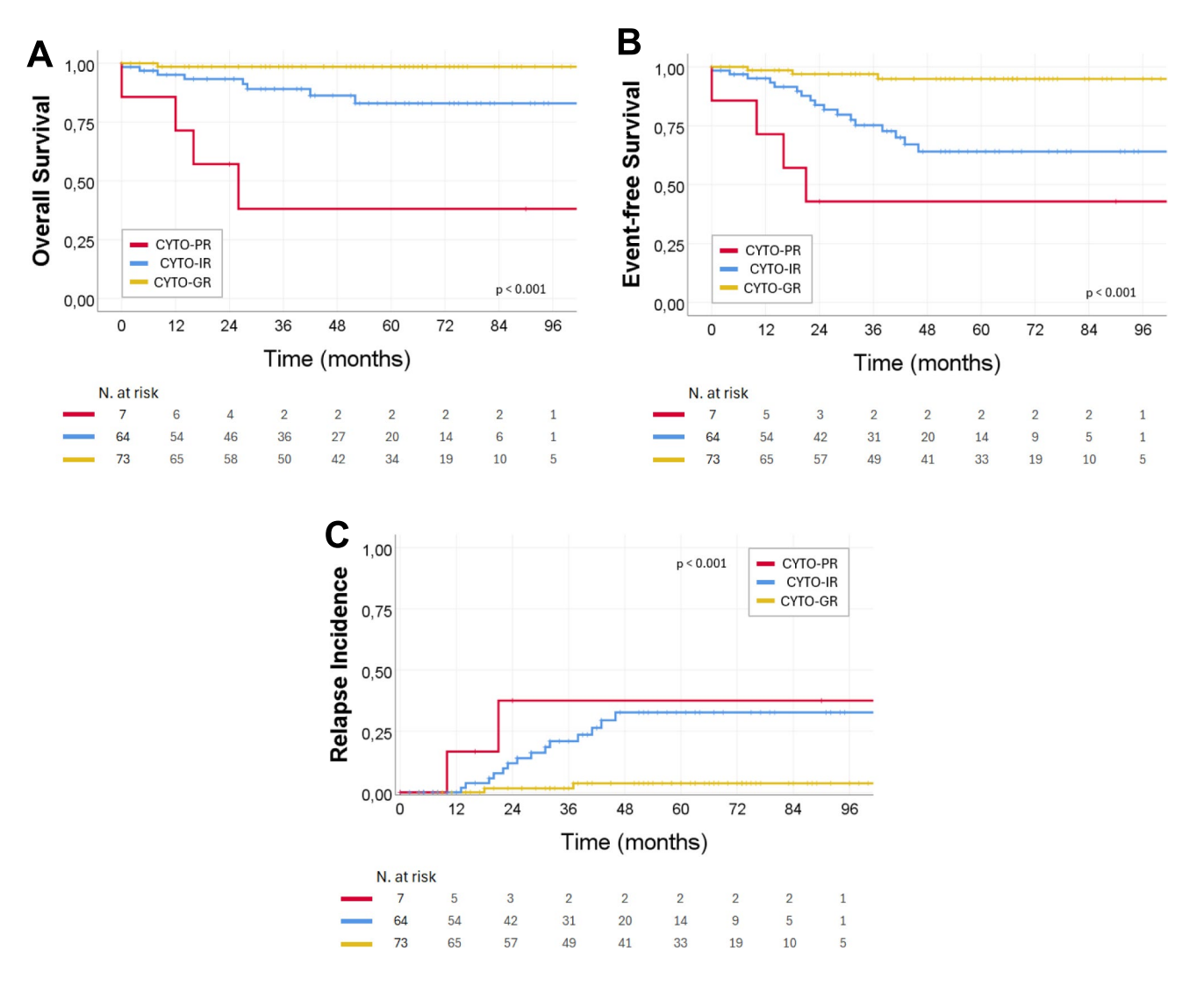


Fig. 5 Outcomes according to the genetic risk classification for our cohort of pediatric B-ALL. (A-C) Kaplan-Meier survival curves showing the overall survival, event-free survival and relapse

incidence according to genetic classification. CYTO-GR: HeH and ETV6::RUNXI; CYTO-PR: KMT2A-r, BCR::ABL1 or hypodiploidy; CYTO-IR: other genetic subtypes

directly detecting *DUX4* rearrangements remains challenging with the employed methods.

Moreover, the study acknowledges the presence of concurrent recurrent genetic alterations alongside the primary genetic abnormalities, consistent with previous observations [19]. It is important to recognize concurrent alterations to inform the prognosis of patients accurately. For example, in cases of *BCR::ABL1* with hyperdiploidy, the prognosis will be primarily driven by the presence of the *BCR::ABL1* abnormality, regardless of the hyperdiploid karyotype. Similarly, identifying *CRLF2*-r alongside iAMP21, *ETV6::RUNX1*, or other *BCR::ABL1*-like fusions is crucial for proper patient classification and risk stratification according to their primary alteration.

Regarding secondary alterations, deletions in genes of interest were observed in 60% of our cohort. The most

common CNAs included deletions in ETV6 and 9p (encompassing CDKN2A/B and PAX5) and IKZF1 deletions, similar to previous reports [20, 21]. The association between the deleted genes and the underlying genetic subtype is also consistent with the literature [21], with IKZF1, PAX5, and PAR1 deletions observed in BCR::ABL1-like patients, PAX5 and CDKN2A/B deletions in B-other patients, and ETV6 deletions in ETV6::RUNX1 patients. Interestingly, our study identified a novel association between RB1 deletion and the ZNF384-r subgroup, which has not been widely reported. Although RB1 deletion was observed in 33% of our ZNF384-r cohort (n=2), it did not correlate with a poorer prognosis in these cases, which contrasts with previous reports linking RB1 deletions to adverse outcomes in other contexts [13, 21]. These findings underscore the need for further investigation into the potential role of RB1 deletions in ZNF384-r patients.



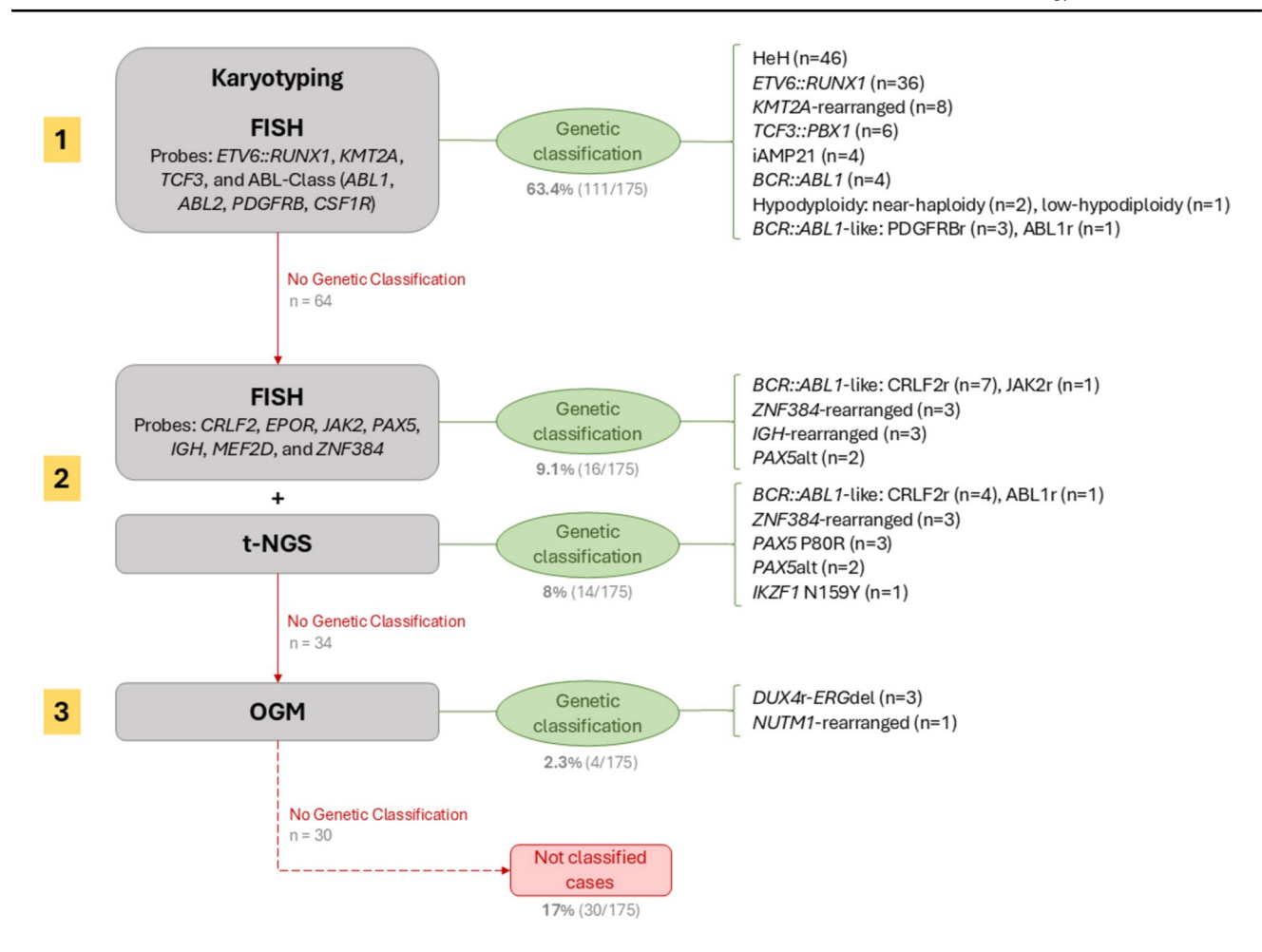


Fig. 6 Genetic Diagnostic Workflow Algorithm for B-ALL. In suspected cases of B-ALL, our recommended diagnostic approach for accurate genetic characterization includes: Step 1, karyotyping and FISH screening for common genetic abnormalities such as ETV6::RUNX1, KMT2A, TCF3, and ABL-class gene fusions (ABL1, ABL2, PDGFRB, CSF1R). Based on our findings, this initial step achieved a genetic diagnosis in 63.4% of cases, effectively identifying high hyperdiploidy (HeH), ETV6::RUNX1, KMT2A-rearranged, TCF3::PBX1, iAMP21, BCR::ABL1, and some BCR::ABL1-like fusions (PDGFRB, ABL1). Step 2 involves an extended FISH panel

for additional probes (*CRLF*2, *EPOR*, *JAK2*, *PAX5*, *IGH*, *MEF2D*, *ZNF384*) and targeted NGS (t-NGS). This step helped identify *BCR::ABL1*-like rearrangements, including *CRLF2-r* and *JAK2-r*, as well as rearrangements of *ZNF384*, *IGH*, and *PAX5* alterations, achieving a genetic diagnosis in 9.1% of cases via FISH and 8% via t-NGS. Step 3, optical genome mapping (OGM), was applied to the remaining undiagnosed cases, leading to the identification of *DUX4r-ERGdel* and *NUTM1* rearrangements in 2.3% of cases. Overall, this stepwise approach was able to achieve a genetic diagnosis in 83% of our cases, leaving 17% undiagnosed after applying all methods

B-ALL in our study displayed a low number of mutations (median 2), which is fewer than the median of four putative somatic driver alterations described by Brady et al. [19]. *PAX5*alt, HeH, and *DUX4*-r showed the highest number of mutations (median 3.5-3). The most frequent mutations found in our B-ALL cohort were *KRAS*, *NRAS*, and *PAX5*, similar to previous reports [19]. Furthermore, we found a specific association between the genetic subtype and mutations, such as *CRLF2*-r with *JAK2* and *ZNF384*-r with *EGFR* and *EZH2*. *TP53* and *NT5C2* mutations were found in 16% of relapsed patients, even though the majority had a favorable prognosis genetic group (HeH and *ETV6*::*RUNX1*), corroborating the association of these mutations with resistance to chemotherapy [22, 23].

Our analysis confirms the critical role of genetics in prognosis. Patients with good-risk (CYTO-GR) genetics had excellent survival rates, while poor-risk (CYTO-PR) patients had worse outcomes. Interestingly, the intermediate risk group within SEHOP-PETHEMA2013 protocol had a high OS (97%), regardless of genetics, suggesting accurate patient stratification based on response to treatment (MRD) and age. However, within this group, the *CRLF2*-r subgroup had a poorer prognosis with a lower EFS and higher relapse rate, while *ZNF384*-r and *PAX5* P80R subgroups showed favorable outcomes, differing from previously described intermediate risk cases [15]. Despite what is described in the literature [13, 20], CNAs did not show significant prognostic differences in survival rates in our cohort, likely due to



the small number of patients. Furthermore, unlike in adults [24], CK presence did not exhibit independent prognostic significance in our pediatric cohort.

In conclusion, this study reinforces the importance of integrated genetic diagnostics for accurate subtyping and prognostication in pediatric B-ALL. Identification of a novel subtype and characterization of secondary abnormalities, provide deeper insights into B-ALL biology, paving the way for personalized treatment approaches. The development of cost-effective strategies to incorporate comprehensive genetic profiling into routine clinical practice is essential. This study highlights the importance of integrating multiple diagnostic techniques for precise genetic diagnosis in pediatric B-ALL, confirming that conventional methods, combined with t-NGS, enable a rapid and accurate diagnosis.

Supplementary Information The online version contains supplementary material available at https://doi.org/10.1007/s00277-024-06151-7.

Author contributions G.HG. and M.O. was responsible for the conception and design of the study. G.HG., B.TV., C.P., S.S., N.MM. and M.O. conducted the laboratory work. G.HG. and B.TV. performed and interpreted the NGS analysis. G.HG. and V.N. performed and revised the statistical analysis. L.M., P.V., T.M. and C.D. were responsible for the patients and performed clinical evaluations. G.HG., M.O., G.A. and F.B. discussed the results. G.HG. prepared the final manuscript for publication. All authors read and approved the final manuscript.

Funding This work was supported by the FERO Foundation under Grant 3281.

Data Availability No datasets were generated or analysed during the current study.

Declarations

Ethical approval All patients provided informed consent in accordance with protocols approved by Institutional Ethics Committee of Vall d'Hebron University Hospital and in compliance with the Declaration of Helsinki.

Competing interest The authors declare no competing interests.

Open Access This article is licensed under a Creative Commons Attribution-NonCommercial-NoDerivatives 4.0 International License, which permits any non-commercial use, sharing, distribution and reproduction in any medium or format, as long as you give appropriate credit to the original author(s) and the source, provide a link to the Creative Commons licence, and indicate if you modified the licensed material. You do not have permission under this licence to share adapted material derived from this article or parts of it. The images or other third party material in this article are included in the article's Creative Commons licence, unless indicated otherwise in a credit line to the material. If material is not included in the article's Creative Commons licence and your intended use is not permitted by statutory regulation or exceeds the permitted use, you will need to obtain permission directly from the copyright holder. To view a copy of this licence, visit http://creativecommons.org/licenses/by-nc-nd/4.0/.

References

- Alaggio R, Amador C, Anagnostopoulos I et al (2022) The 5th edition of the World Health Organization Classification of Haematolymphoid Tumours: Lymphoid Neoplasms. Leukemia. https:// doi.org/10.1038/s41375-022-01620-2
- Schwab C, Harrison CJ (2018) Advances in B-cell precursor acute lymphoblastic leukemia genomics. Hemasphere 2:1–9. https://doi. org/10.1097/HS9.0000000000000053
- Zaliova M, Stuchly J, Winkowska L et al (2019) Genomic landscape of pediatric B-other acute lymphoblastic leukemia in a consecutive European cohort. Haematologica 104:1396–1406. https:// doi.org/10.3324/haematol.2018.204974
- Gu Z, Churchman ML, Roberts KG et al (2019) PAX5-driven subtypes of B-progenitor acute lymphoblastic leukemia. Nat Genet 51:296–307. https://doi.org/10.1038/s41588-018-0315-5
- Schwab CJ, Murdy D, Butler E et al (2022) Genetic characterisation of childhood B-other-acute lymphoblastic leukaemia in UK patients by fluorescence in situ hybridisation and Multiplex Ligation-dependent Probe Amplification. Br J Haematol 196:753–763. https://doi.org/10.1111/bjh.17869
- Li JF, Dai YT, Lilljebjörn H et al (2018) Transcriptional landscape of B cell precursor acute lymphoblastic leukemia based on an international study of 1,223 cases. Proc Natl Acad Sci U S A 115:E11711–E11720. https://doi.org/10.1073/pnas.1814397115
- Duncavage EJ, Bagg A, Hasserjian RP et al (2022) Genomic profiling for clinical decision making in myeloid neoplasms and acute leukemia. Blood 140:2228–2247. https://doi.org/10.1182/blood. 2022015853
- Rack K, De Bie J, Ameye G et al (2022) Optimizing the diagnostic workflow for acute lymphoblastic leukemia by optical genome mapping. Am J Hematol 97:548–561. https://doi.org/10.1002/ajh. 26487
- Badell I, Díaz de Heredia C, Dapena JL et al (2014) Recomendaciones terapéuticas LAL/SEHOP-PETHEMA 2013
- Hidalgo-Gómez G, Palacio-Garcia C, Gallur L et al (2021) Is acute lymphoblastic leukemia with mature B-cell phenotype and KMT2A rearrangements a new entity? A systematic review and meta-analysis. Leuk Lymphoma 62:2202–2210. https://doi.org/ 10.1080/10428194.2021.1907375
- Zaliova M, Potuckova E, Hovorkova L et al (2019) ERG deletions in childhood acute lymphoblastic leukemia with DUX4 rearrangements are mostly polyclonal, prognostically relevant and their detection rate strongly depends on screening method sensitivity. Haematologica 104:1407–1416. https://doi.org/10.3324/haematol. 2018.204487
- Rehn JA, O'connor MJ, White DL, Yeung DT (2020) DUX hunting—clinical features and diagnostic challenges associated with DUX4-rearranged leukaemia. Cancers (Basel) 12:1–15
- Hamadeh L, Enshaei A, Schwab C et al (2019) Validation of the United Kingdom copy-number alteration classifier in 3239 children with B-cell precursor ALL. Blood Adv 3:148–157. https:// doi.org/10.1182/bloodadvances.2018025718
- Qian M, Cao X, Devidas M et al (2018) TP53 Germline Variations Influence the Predisposition and Prognosis of B-Cell Acute Lymphoblastic Leukemia in Children. J Clin Oncol 36:591–599. https://doi.org/10.1200/JCO
- Schwab C, Cranston RE, Ryan SL et al (2023) Integrative genomic analysis of childhood acute lymphoblastic leukaemia lacking a genetic biomarker in the UKALL2003 clinical trial. Leukemia 37:529–538. https://doi.org/10.1038/s41375-022-01799-4



- Tueur G, Quessada J, De Bie J et al (2023) Cytogenetics in the management of B-cell acute lymphoblastic leukemia: Guidelines from the Groupe Francophone de Cytogénétique Hématologique (GFCH). Curr Res Transl Med 71:103434. https://doi.org/10. 1016/j.retram.2023.103434
- Iacobucci I, Kimura S, Mullighan CG (2021) Clinical Medicine Biologic and Therapeutic Implications of Genomic Alterations in Acute Lymphoblastic Leukemia. J Clin Med 10:3792. https://doi. org/10.3390/jcm
- Inaba H, Mullighan CG (2020) Pediatric acute lymphoblastic leukemia. Haematologica 105:2524–2539
- Brady SW, Roberts KG, Gu Z et al (2022) The genomic landscape of pediatric acute lymphoblastic leukemia. Nat Genet 54:1376– 1389. https://doi.org/10.1038/s41588-022-01159-z
- Song Y, Fang Q, Mi Y (2022) Prognostic significance of copy number variation in B-cell acute lymphoblastic leukemia. Front Oncol 12. https://doi.org/10.3389/fonc.2022.981036
- 21. Steeghs EMP, Boer JM, Hoogkamer AQ et al (2019) Copy number alterations in B-cell development genes, drug resistance, and

- clinical outcome in pediatric B-cell precursor acute lymphoblastic leukemia. Sci Rep 9. https://doi.org/10.1038/s41598-019-41078-4
- Hof J, Krentz S, Van Schewick C et al (2011) Mutations and deletions of the TP53 gene predict nonresponse to treatment and poor outcome in first relapse of childhood acute lymphoblastic leukemia. J Clin Oncol 29:3185–3193. https://doi.org/10.1200/JCO. 2011.34.8144
- Dieck CL, Ferrando A (2019) Genetics and mechanisms of NT5C2-driven chemotherapy resistance in relapsed ALL. Blood 133:2263–2268. https://doi.org/10.1182/blood-2019-01-852392
- Moorman AV, Barretta E, Butler ER et al (2022) Prognostic impact of chromosomal abnormalities and copy number alterations in adult B-cell precursor acute lymphoblastic leukaemia: a UKALL14 study. Leukemia 36:625–636. https://doi.org/10.1038/ s41375-021-01448-2

Publisher's Note Springer Nature remains neutral with regard to jurisdictional claims in published maps and institutional affiliations.

